Microstrip resonator for nonlinearity investigation of thin magnetic films and magnetic frequency doubler

B. A. Belyaev, A. O. Afonin, A. V. Ugrymov, I. V. Govorun, P. N. Solovev, and A. A. Leksikov

View Online   Export Citation   CrossMark

ARTICLES YOU MAY BE INTERESTED IN
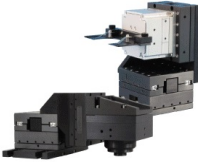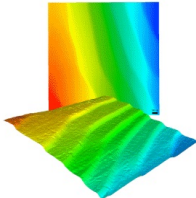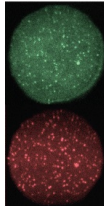
Nanopositioning Systems

Modular Motion Control

AFM and NSOM Instruments

Single Molecule Microscopes

MCL
MAD CITY LABS INC.
www.madcitylabs.com

AIP Publishing

Microstrip resonator for nonlinearity investigation of thin magnetic films and magnetic frequency doubler

View Online   Export Citation   CrossMark

B. A. Belyaev,[1,2] [iD] A. O. Afonin,[1] [iD] A. V. Ugrymov,[1] [iD] I. V. Govorun,[1] [iD] P. N. Solovev,[1] [iD]
and A. A. Leksikov[1,a] [iD]

AFFILIATIONS

[1] Kirensky Institute of Physics SB RAS, Krasnoyarsk 660036, Russia
[2] Siberian Federal University, Krasnoyarsk 660041, Russia

[a] Author to whom correspondence should be addressed: a.a.leksikov@gmail.com

ABSTRACT

A structure that consists of a $\lambda/4$ stepped-impedance microstrip resonator is proposed as an instrument for the investigation of nonlinear effects in thin magnetic films and also can be used as a microwave frequency doubler. A conversion efficiency of 0.65% is observed at a one-layer 100 nm $Ni_{80}Fe_{20}$ thin film at an input signal level of 4.6 W for a 1 GHz probe signal. The maximum measured conversion efficiency (1% at 1 GHz) was achieved for the 9-layer $Ni_{80}Fe_{20}$ film where 150 nm magnetic layers were separated by SiO_2 layers.

Published under license by AIP Publishing. https://doi.org/10.1063/5.0009045

I. INTRODUCTION

Despite that recently most commercial microwave multipliers employ semiconductor elements as nonlinear media for generation of high-order harmonics, a number of applications when semiconductor elements are not suitable still exist. For this reason, great attention is devoted to investigations of new methods and materials, which can be used for multiplier designing,[1–3] for example, graphene[4–6] or ferroelectric films.[7] Magnetic materials are well known as nonlinear media;[8–13] they are well suitable for nonlinear investigations and applications,[14–16] and it is obvious that attempts were made to design magnetic frequency converters.[17,18] At the same time, most of the present investigations are performed at frequencies of spin wave mode generation,[8] which will be promising in the future but are rather high for modern electronics.

Recently, mainly two methods are exploited for excitation in magnetic media of nonlinear harmonics using microwave fields. The most common method, a method of broadband stripline spectroscopy,[19–25] is the same as for ferromagnetic resonance (FMR) investigations, when a microstrip or a coplanar line is used for RF-field generation. The main advantage of the method is that the line is not a frequency selective structure, so it can be easily simulated and used in a very wide frequency range, allowing one to use it as a

generator and detector of nonlinear harmonics simultaneously and making it the most common method for the investigation of spin waves traveling in magnetic films.

In the other method,[26,27] independent excitation and detection circuits are used. For example, in Ref. 27, for excitation, an X-band waveguide was employed to excite the second harmonics in a YIG sample, while detection was performed by a K-band waveguide. The main advantage of the method is that the frequency of the excitation signal is lower than the cut-off frequency of the receiver waveguide which means that most of the energy transmitted to the ferrite element will be transferred to the nonlinear oscillation modes. However, two remarks should be made about the above-mentioned method. Any regular waveguide is transparent for high-order harmonics of its principal eigenmode, meaning that all high-order harmonics excited in the ferrite will also be transferred to the receiver waveguide. In other words, the energy transferred to the ferrite can be involved in the excitation of all nonlinear harmonics, reducing the efficiency of the device with the second harmonic generation. In addition, a frequency doubler in waveguide implementation will be tremendous in size for L- and S-bands, which is the scope of the current investigation. This problem can be solved, if one would apply planar electrodynamic resonators, for example, microstrip or stripline resonators. These structures are common in

VHF and UHF ranges in communication systems as a part of system components because of their diminutiveness and suitable quality factor. For this reason, much attention was paid to the resonator structure in the presence of the magnetic material, particularly, frequency tuning vs a magnetic state of a material[28–31] as the resonators are prospective in terms of application in active tunable microwave devices.[32–34]

In the resonator method, one resonator is used to excite the media and to measure its nonlinearity by transferring high-order harmonics to the output of the device. The main advantage of this method is that it operates in the standing wave mode, meaning that the energy stored in the resonator will be proportional to its loaded quality factor. Hence, much more energy will be available to excite nonlinearity in the media. It is well known that a regular microstrip resonator has an equidistant spectrum of eigenfrequencies, so it has the same disadvantage as the waveguide method. However, the incorporation of steps in the width of the resonator allows one to displace the eigenfrequency of resonant oscillation modes. In addition, in the best case, presented in the current investigation, the frequency of the second oscillation mode will be twice the frequency of the first mode, while frequencies of the 3rd and 4th modes will be shifted to much higher frequencies. Hence, most of the energy injected in the resonator will be used to derive a signal of the second harmonics. A brief explanation of the nonlinear effect is presented in Sec. II. The proposed resonator construction for the investigation of the nonlinearity of magnetic media will be presented in Sec. III. The experimental setup will be discussed in Sec. IV, while the experimental results for $Ni_{80}Fe_{20}$ thin magnetic films will be presented in Sec. V. The results of the investigation are summarized in Sec. VI.

II. FREQUENCY DOUBLING IN A MAGNETIC MEDIUM

The dynamics of the magnetization **M** are described by the Landau–Lifshitz equation,

$$\frac{\partial \mathbf{M}}{\partial t} = -\gamma \mathbf{M} \times \mathbf{H}^{\text{eff}} + \frac{\alpha}{M} \mathbf{M} \times \frac{\partial \mathbf{M}}{\partial t}, \quad (1)$$

where γ is the gyromagnetic ratio, α is the damping parameter, M is the saturation magnetization, and $\mathbf{H}_{\text{eff}}$ is an effective field, usually composed of three different terms: the applied constant and time-varying magnetic fields, the shape demagnetizing field, and the magnetic anisotropy field. In an equilibrium state, the magnetization vector is oriented along the effective field ($\mathbf{M} \times \mathbf{H}_{\text{eff}} = 0$). In the case of an isotropic magnet under the influence of a circularly polarized microwave field h with components h_x and h_y applied in the x–y plane perpendicular to the $\mathbf{H}_{\text{eff}}$ vector at frequency ω, the magnetization vector will precess about $\mathbf{H}_{\text{eff}}$ at the frequency of the exiting field in a circular orbit in the x–y plane. In this case, the amplitudes of the dynamic time dependent part $\mathbf{m}(t)$ of the magnetization vector **M** are $|m_x| = |m_y|$ and $|m_z| = 0$ [Fig. 1(a)]. However, if the magnet is anisotropic or the driving microwave field is linearly polarized, the magnetization oscillation in the x–y plane may become elliptical ($|m_x| \neq |m_y|$). However, since the magnetization vector length must be constant, the non-zero m_z component will emerge [Fig. 1(b)]. From this simplified picture readily follows that m_z varies at a doubled frequency 2ω of the excitation field.[26]
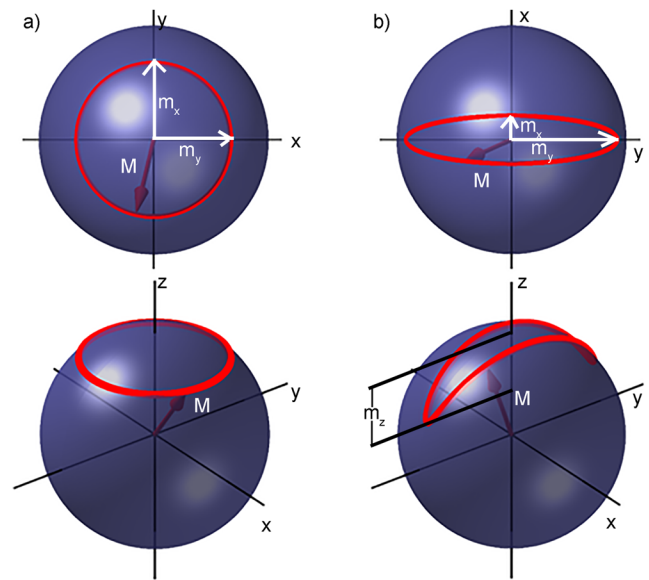

FIG. 1. Sketch of magnetization dynamics: (a) an isotropic magnet excited by the circularly polarized microwave field ($|m_x| = |m_y|$) and (b) an anisotropic magnet excited by the linearly polarized field ($|m_y| > |m_x|$). In the second case, a double frequency component of magnetization m_z arises.

Using the second-order approximation, the amplitude of the double frequency component m_z can be expressed as

$$m_z = \frac{1}{4M} \left| m_x^2 - m_y^2 \right|, \quad (2)$$

where $m_x = \chi_{xx}(\omega)h_x + i\chi_{xy}(\omega)h_y$ and $m_y = i\chi_{yx}(\omega)h_x + \chi_{yy}(\omega)h_y$ are the components of the dynamic magnetization determined from the solution of the linearized Landau–Lifshitz equation with χ_{xx}, χ_{xy}, χ_{yx}, and χ_{yy} being the components of the magnetic susceptibility tensor.[35] In general, the magnitude of the magnetic susceptibility reaches its maximum when the frequency of the excitation field is close to the ferromagnetic resonance frequency of the magnet. The expression (2) shows why a thin magnetic film is a preferred medium for the excitation of nonlinear magnetization dynamics: Because of the film's shape magnetic anisotropy, it demonstrates a very high $|m_y|/|m_x|$ ratio (x-axis being normal to the film plane). From the expression (2) also follows that the frequency doubling in a magnetic medium is a quadratic effect—the output power at frequency 2ω increases quadratically with the input power at frequency ω. Concluding this section, we should note that the general solution of the inherently nonlinear Landau–Lifshitz equation reveals rather complex dynamics of magnetization, with the excitation of high-order harmonics with exponentially decreasing amplitudes.[36,37]

III. RESONATOR STRUCTURE

The microstrip resonator is a well-known instrument for material investigation.[38] $\lambda/2$ microstrip resonators are easier in fabrication and usually have a higher measured unloaded quality factor than $\lambda/4$ microstrip resonators, which are twice smaller than the
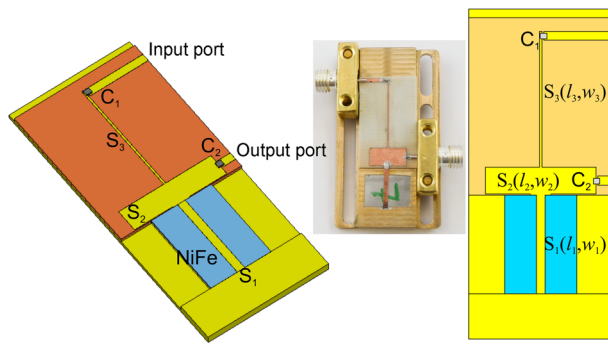
FIG. 2. Resonator construction and its photo in the middle.

first mentioned. This state is very important in terms of the fabrication of a frequency doubler for a commercial microwave system. However, a regular $\lambda/4$ microstrip resonator has a frequency of the second oscillation mode equal to $3f_0$ (f_0—frequency of the fundamental oscillation mode), so one will need to make irregularities in the resonator strip to shift the frequency of the second oscillation mode to a frequency of $2f_0$.

In Fig. 2, the structure of the proposed microstrip resonator for the investigation of nonlinear dynamics of thin magnetic films is presented, which can be used as a base for a magnetic frequency doubler. The resonator is divided into two parts: one (S_1) that is closer to the grounded end of the strip has an air-gapped structure, where a substrate with a film under investigation is placed below the strip, while the second part is a stepped impedance microstrip resonator designed on a dielectric substrate. The thickness of the air gap and the length of the segment of the resonator are strongly dependent on parameters of a thin magnetic film, particularly on the size of the dielectric substrate used in film synthesis. The width of the resonator segment at the air-gapped part is taken as an optimum between the current density in the strip and the amount of magnetic material involved in the harmonic generation, and in our case, when the size of a film is 8×11 mm^2, it is equal to 1.0 mm. It means that frequencies of resonator's modes can be tuned only by changing parameters of the microstrip part of the structure, particularly, the width and the length of segments S_2 and S_3 (w_2, w_3, l_2, and l_3).

To investigate the generation of the second harmonics in a magnetic film, one will need to shift the frequency of the second oscillation mode to a double frequency of the principal oscillation mode ($2f_0$). It can be obtained by making a step of the width of the segments S_2 and S_3 ($w_2 > w_3$). It should be noted that, in the best case, the middle of the segment S_2 should be situated in the antinode of the electric field as the output of the resonator is also connected to the middle of the segment through a SMD capacitor. This solution will allow one to isolate the output of the resonator from the excitation signal. It is obvious that a change in the width of the segments will lead to a change in the frequency of the first mode of the resonator, which can be tuned by lengths l_2 and l_3, whereas parameters w_1 and l_1 are fixed. Another feature of the resonator is that the step of the width that shifts even modes to a lower frequency also shifts odd modes to a higher frequency, thereby breaking the frequency multiplicity and the equidistance of the oscillation modes in the resonator. In terms of the nonlinearity investigations, this means that

the system will be sensitive only for the second harmonics generated in a film, and all other modes, allowed for generation in the film, are prohibited for the resonator.

The resonator is connected to the input port at the open end of the segment S_3, ensuring that it has a proper matching with feedlines at a frequency of the principal oscillation mode. The overall degree of matching is determined by the value of capacitance of the SMD capacitor used to connect with the excitation port.

For the current investigation, a resonator with the frequency of the principal oscillation mode equal to 1 GHz was designed and fabricated. The parameters of the resonator were as follows: w_1 = 1.0 mm, w_2 = 9 mm, w_3 = 0.3 mm, l_1 = 12 mm, l_2 = 2.7 mm, and l_3 = 24.1 mm. A 0.508 mm Rogers RO4003B was used as a dielectric substrate for stepped impedance segments of the resonator. The width of the feedlines connecting the external ports with the capacitors is 1.1 mm, which correspond to the 50 Ω impedance of the microstrip lines fabricated on the substrate. A value of the capacitance of SMD components was obtained during the measurements, and it was found that in terms of the second harmonics excited in the film and transferred to the output of the device, the feedlines should be connected to the resonator using 1 pF capacitance. An increase and a decrease in the capacitance lead to a decrease in the level of the second harmonics emerging the device, which is explained by the existence of an optimum degree of matching with feedlines. An increase in the matching degree decreases the loaded Q-factor of the resonator, meaning that less energy can be transferred to a film from the resonator for the harmonic generation in one period of time. On the other hand, a decrease in the matching degree, which increases the value of the Q-factor, reduces the overall level of energy transmitted through the resonator due to enlarged reflected power from the resonator.
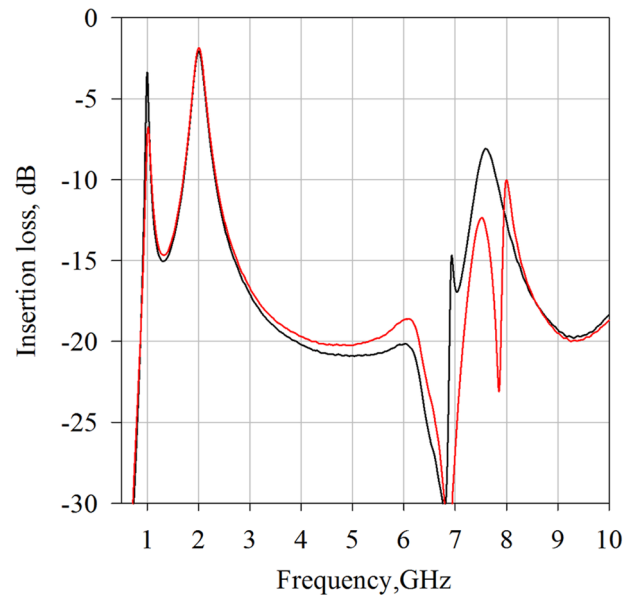

FIG. 3. Resonator frequency response in the absence of a magnetic film (black line) and in the case of the harmonic generation (red line).

The frequency dependence of the fabricated resonator is presented in Fig. 3, in the absence of a magnetic film and in the state of the second harmonic generation. It can be seen that in the state of the harmonic generation, the frequency of the second oscillation mode of the resonator exactly doubles (2 GHz) the frequency of the principal mode (1 GHz) at which the film is excited. At the same time, the frequency of the third oscillation mode is 5.5 GHz, which suggests that the one nonlinear harmonic was excited in the structure.

IV. MEASUREMENT SETUP

To purify the probe signal and in order not to overload the input circuit of the spectrum analyzer used to measure the signal, two bandpass filters were designed and fabricated. The first one, connected to the input of the resonator, has a passband at the frequency of the first oscillation mode of the resonator, while the frequencies of the second, the third, and the fourth modes are located inside the stopband of the filter. The filter's task is to purify a probe signal, by filtering harmonic and non-harmonic components of the signal at the output of a microwave generator, which are further additionally amplified before the resonator. The second filter has a passband at the frequency of the nonlinear harmonic under investigation, while the frequency of the probe signal and frequencies of another harmonic signal are located in the stopband of the filter. The filter locks the probe signal in the resonator forcing it to transform into a nonlinear harmonic. In addition, the filter is protecting the input circuit of a spectrum analyzer from a probe signal and allows one to make a proper measurement of a harmonic level.

First of all, let us consider how a high-level probe signal influences the input schemes of spectrum analyzers and distorts the level of the signal under investigation. A 20 dBm probe signal was used in two schemes that differ from each other only by the second bandpass filter installed at the output of the resonator filled with a clear quartz substrate. One can see from Fig. 4 that the spectrum of the probe signal (black line) consists of harmonics generated and amplified before the resonator, as it has been previously mentioned. Next, the measured signal is strongly distorted in terms of increased noise level for frequencies less than 3 GHz. The inclusion of the second filter reduces the level of the signal at 1 GHz on 76 dB and at 3 GHz on 100 dB, and, what is more important, a
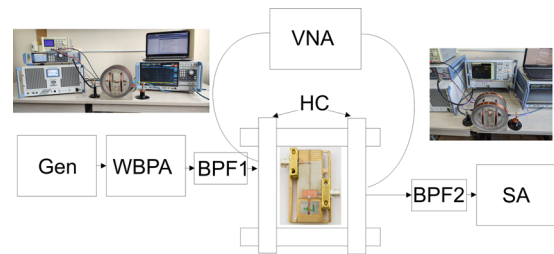

FIG. 5. Measurement setup. HC—Helmholtz coil, VNA—vector network analyzer R&S ZVA50, Gen—microwave generator R&S SMA100B, WBPA—wideband power amplifier R&S BBA150, BPF1—bandpass filter 1, BPF2—bandpass filter 2, and SA—spectrum analyzer R&S FSW.

19 dB decrease of the signal level of the second harmonics is observed, which is much closer to a specified level for the generator (>60 dBc) [Fig. 4(a)].

The connection of the first bandpass filter before the resonator reduces the harmonic level in the probe signal on 85 dB, as it can be seen from Fig. 4(b), so one can be sure about the purity of the probe signal.

The presented method was previously[39] used to investigate the nonlinear behavior of a plasma antenna and, for the first time, allowed to confirm that plasma antennas are strictly nonlinear devices, previously presented results left questions and doubts about the nature of the measured harmonics.

The whole scheme of the investigation is presented in Fig. 5; it consists of two parts, one with a vector network analyzer as the main sensitive instrument, which is used to measure the resonator frequency response and make a slight frequency tuning, in the presence of magnetic materials, and the tuning of the filters in the presence of the resonator. The second part of the scheme is the standard scheme for nonlinearity investigations, which consists of a microwave generator, a broadband microwave power amplifier, and a spectrum analyzer. An external magnetic field used for biasing a thin film under investigation is produced by two orthogonal Helmholtz coils that allow obtaining the angular dependence of harmonic generation for the fixed resonator and a magnetic film inside it. A comparison
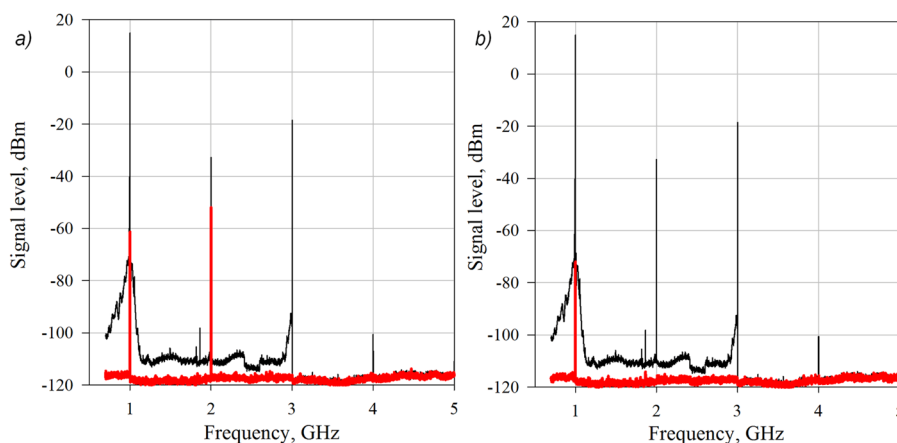

FIG. 4. Probe signal spectrum measured by the spectrum analyzer (black lines): (a) in the presence of the bandpass filter 2 (red line) and (b) in the presence of the bandpass filters 1 and 2 (red line).
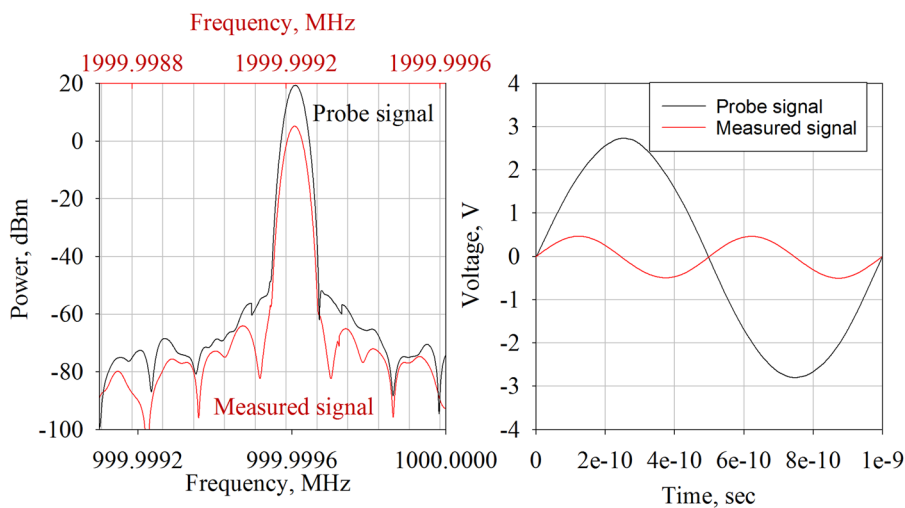
FIG. 6. Comparison of probe (1 GHz) and measured (2 GHz) signals in frequency (left panel) and time (right panel) domains.

of the probe and measured signal is presented in Fig. 6 for frequency (left panel) and time (right panel) domains.

V. EXPERIMENTAL RESULTS

For the current investigation, a 100 nm thin film was deposited from the $Ni_{80}Fe_{20}$ target in the presence of a bias magnetic field in the chamber during a dc-magnetron deposition on a 0.5 mm quartz substrate. An external magnetic field, applied during deposition, induced in the film an in-plane magnetic uniaxial anisotropy. Two samples with lateral size 8 × 11 mm^2 were further cut off from the film so that sample 1 has the easy axis of magnetization (EA) along the short side of the sample, while, in sample 2, the EA was directed along the long side.

As the first step of the investigation, both samples were characterized by means of a local FMR spectrometer[40] to obtain the following magnetic parameters of the film:

For sample 1, H_{FMR} = 8.1 Oe, ΔH_{FMR} = 3.7 Oe, M_s = 914 emu/cm^3, H_k = 2.73 Oe, and T_k = 89.9°.

For sample 2, H_{FMR} = 14 Oe, ΔH_{FMR} = 3.7 Oe, M_s = 917.2 emu/cm^3, H_k = 2.96 Oe, and T_k = 1.7°.

Here, H_{FMR} is the field of ferromagnetic resonance, ΔH_{FMR} is the resonance linewidth, M_s is the saturation magnetization, H_k is the anisotropy field, and T_k is the angle of the easy axis.

In Fig. 7, the results for the level of the second harmonics vs the angle of the external field are presented at the level of the probe signal limited to 100 mW. The measurements were performed at the field being higher than the anisotropy field obtained during FMR spectrum investigation. Figure 7 consists of the four curves:

1. yellow curve: sample 1 short side oriented along the strip;
2. green curve: sample 1 long side oriented along the strip;
3. black curve: sample 2 short side oriented along the strip;
4. red curve: sample 2 long side oriented along the strip.

One can see from Fig. 7 that the maximum level of the second harmonics is observed, when induced magnetic anisotropy and shape anisotropy give the same contribution to the harmonic generation (red curve), while the smallest one is observed when the anisotropies are in opposition (black curve). At the same time, the

shape anisotropy gives a higher contribution than the induced one, according to the difference between the maximum levels in the yellow and black curves.

The maximum of harmonic generation is observed at an angle of 25° from the hard axis. This behavior of the angular dependencies can be explained as follows: when the film is placed in the resonator so that the direction of the induced anisotropy (EA) is oriented along the resonator strip and the external field is applied perpendicular to it, the coupling between the resonator and magnetic layer is rather small, allowing magnetic dynamics in the film to develop independently with the minimum influence of the resonator, which brings the system to the highest quality factor, which is proved by a narrow linewidth. In addition, in such a configuration, a bigger amount of magnetic material is incorporated in the harmonic generation, as the shape anisotropy is directed along the resonator strip.

On the opposite, when the EA of the induced anisotropy is directed along the microwave field from the resonator, the resonator
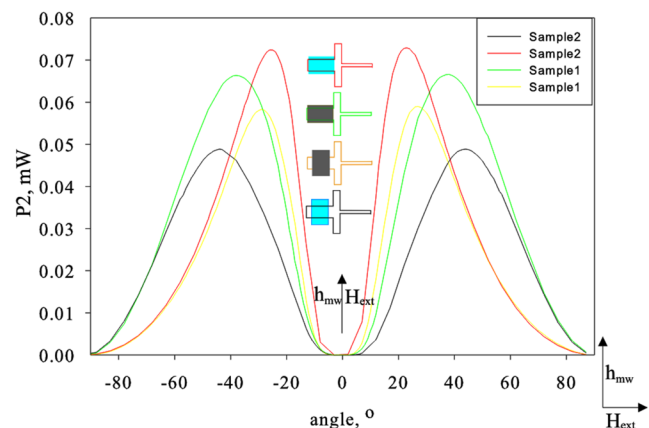

FIG. 7. Angular dependences of the harmonic generation for both the samples.
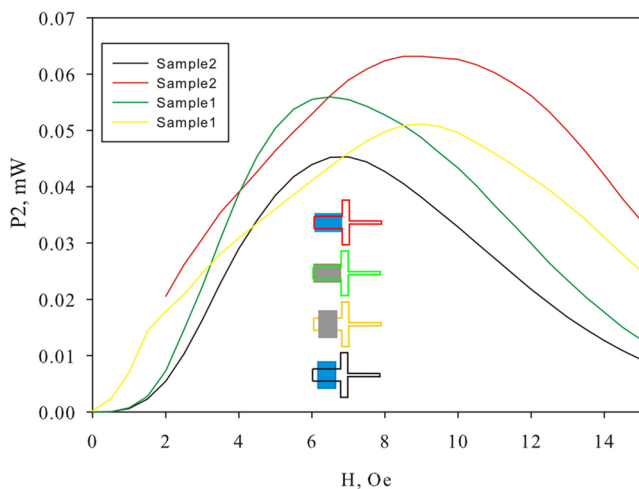
FIG. 8. Field dependences of the harmonic generation for both the samples.

FIG. 10. Conversion efficiency of the second harmonics vs input power for the 9-layer $Ni_{80}Fe_{20}$ film.

has a maximum coupling with the film, reducing the quality factor of generation and decreasing the overall level of harmonics.

Next, the behavior of black and green curves displays that the volume of the magnetic material, which can be incorporated in the harmonic generation, contributes more than the magnetic state in a film.

For the optimal angles, obtained from Fig. 7 (47°—black curve, 25°—red curve, 40°—green curve, 30°—yellow curve), the field dependences of the level of the second harmonics were measured, which are presented in Fig. 8. One can see that the results obtained for the angle dependence are proved for the field dependence: The maximum of the harmonic level is observed for the case when the
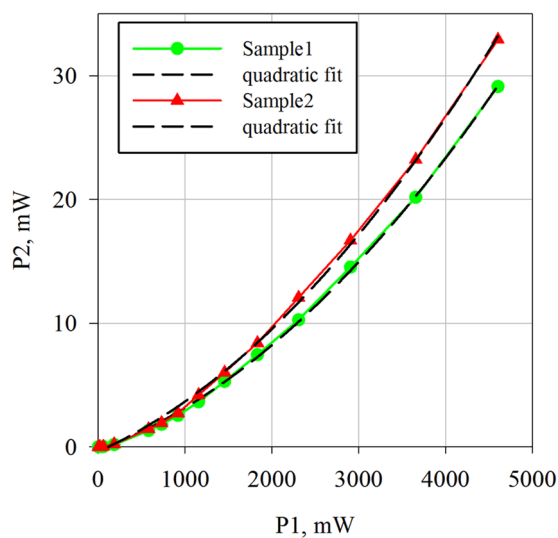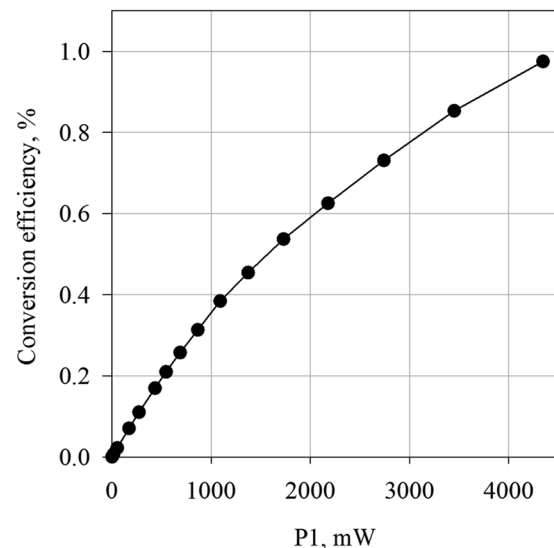
shape and induced anisotropies have the same contribution; at the same time, the magnetic field, which corresponds to the maximum harmonic level, is 1.5 times higher (9 Oe for red curve) than for the case where anisotropies have different contributions, as the direction of the applied external field is closer to the hard axis of the film.

The power dependencies of the harmonic generation for the two best cases were obtained for the optimal amplitude and the angle of the applied field (9 Oe/25°—sample 1, 6 Oe/40°—sample 2), which are presented in Fig. 9. The classical quadratic behavior of the power dependence is observed, where, for low powers, the level of the second harmonics does not change much, and at powers above 1 W, there is a significant increase in the harmonic level.

The maximum measured harmonic level for the presented magnetic films is 30 mW for the probe signal of 4.6 W, which corresponds to a conversion efficiency of 0.65% at 1 GHz. For the moment, the maximum observed conversion efficiency of the second harmonics was measured for the 9-layer $Ni_{80}Fe_{20}$ film where 150 nm magnetic layers were separated by SiO_2 layers and were found to be 1% (43 mW for a probe signal of 4.2 W), whose conversion efficiency vs input power is presented in Fig. 10.

VI. CONCLUSIONS

A construction of a λ/4 stepped-impedance microstrip resonator based on a hybrid substrate, which has an air gap in the area of the grounded end, designed to install a dielectric substrate containing a thin magnetic film on its surface is presented. Near the field of ferromagnetic resonance in the film, the high-frequency field of the strip resonator gives rise to a nonlinear regime of magnetization oscillations in the film, which causes the generation of a high-frequency current in the resonator at a double frequency. The proposed structure can be used either for the investigation of nonlinear effects in magnetic films or magnetic samples or as a microwave

FIG. 9. Level of the second harmonics vs input power for both samples and their quadratic fit.

frequency doubler for the case, when semiconductor devices cannot be applied.

A method for nonlinear investigation is proposed based on the application of bandpass filters and the resonator, which allows for the measuring of pure nonlinear effects of a film, but not a measurement setup.

For two 100 nm $Ni_{80}F_{20}$ thin films with different magnetic configurations, but deposited during the same dc-magnetron deposition, the way to obtain the maximum of the second harmonic generation (a conversion efficiency of 0.65% at 1 GHz) is presented.

The maximum conversion efficiency (1%) measured at the 1 GHz probe signal was achieved with the 9-layer $Ni_{80}Fe_{20}$ film where 150 nm magnetic layers were separated by SiO_2 layers.

ACKNOWLEDGMENTS

DATA AVAILABILITY

The data that support the findings of this study are available from the corresponding author upon request.

REFERENCES

[1]J. Zhao, V. K. Chillara, B. Ren, H. Cho, J. Qiu, and C. J. Lissenden, J. Appl. Phys. **119**, 064902 (2016).

[2]Y. Shen, J. Gao, Y. Wang, J. Li, and D. Viehland, J. Appl. Phys. **115**, 094102 (2014).

[3]J. C. Booth, K. T. Leong, S. Y. Lee, J. H. Lee, B. Oh, H. N. Lee, and S. H. Moon, Supercond. Sci. Technol. **16**, 1518–1522 (2003).

[4]P. Peng, Z. Tian, M. Li, Z. Wang, L. Ren, and Y. Fu, J. Appl. Phys. **125**, 064503 (2019).

[5]V. A. Margulis and E. E. Muryumin, J. Appl. Phys. **126**, 054301 (2019).

[6]M. Dragoman, A. Cismaru, A. Dinescu, D. Dragoman, G. Stavrinidis, and G. Konstantinidis, J. Appl. Phys. **114**, 154304 (2013).

[7]F. Ponchel, L. Burgnies, D. Ducatteau, É. Lheurette, D. Rémiens, and D. Lippens, J. Appl. Phys. **114**, 194103 (2013).

[8]K. Livesey, Handb. Surf. Sci. **5**, 169–214 (2016).

[9]H. Yan, Q. Wang, and I. Awai, Electron. Lett. **32**(19), 1787–1789 (1996).

[10]Y. K. Fetisov and C. E. Patton, IEEE Trans. Magn. **40**(2), 473–482 (2004).

[11]Y. S. Gui, A. Wirthmann, and C. M. Hu, Phys. Rev. B **80**(18), 184422 (2009).

[12]A. V. Drozdovskii and A. B. Ustinov, Tech. Phys. Lett. **36**(9), 834–837 (2010).

[13]H. Zhou, X. Fan, and L. Ma, Appl. Phys. Lett. **108**(19), 192408 (2016).

[14]Z. Celinski, I. R. Harward, N. R. Anderson, and R. E. Camley, Handb. Surf. Sci. **10**, 421–457 (2016).

[15]M. Bao, A. Khitun, Y. Wu, J.-Y. Lee, K. L. Wang *et al.*, Appl. Phys. Lett. **93**, 072509 (2008).

[16]A. B. Ustinov, A. V. Drozdovskii, and B. A. Kalinikos, Appl. Phys. Lett. **96**, 142513 (2010).

[17]K. Poole and P. Tien, Proc. IRE **46**(7), 1387–1396 (1958).

[18]C. Cheng and W. E. Bailey, Appl. Phys. Lett. **103**, 242402 (2013).

[19]B. A. Kalinikos, IEEE Proc. **127**, 4–10 (1980).

[20]P. R. Emtage, J. Appl. Phys. **53**(7), 5122–5125 (1982).

[21]D. Bhattacharya and N. B. Chakraborti, J. Appl. Phys. **62**(10), 4322–4324 (1987).

[22]J. Barak and U. Lachish, J. Appl. Phys. **65**(4), 1652–1658 (1989).

[23]B. A. Kalinikos, N. G. Kovshikov, and A. N. Slavin, Sov. Phys. JETP **67**(2), 303–312 (1988).

[24]J. W. Boyle, S. A. Nikitov, A. D. Boardman, and K. Xie, J. Magn. Magn. Mater. **173**(3), 241–252 (1997).

[25]H. Benner, B. A. Kalinikos, N. G. Kovshikov, and M. P. Kostylev, JETP Lett. **72**, 2132–2216 (2000).

[26]J. Melchor, W. Ayres, and P. Vartanian, Proc. IRE **45**(5), 643–646 (1957).

[27]E. Kirchner, H. Shaw, and D. Winslow, IEEE Trans. Magn. **2**(4), 691–696 (1966).

[28]W. S. Ishak and K. Chang, IEEE Trans. Microwave Theory Tech. **34**(12), 1383–1393 (1986).

[29]M. Tsutsumi and T. Fukusako, Electron. Lett. **33**(8), 687–688 (1997).

[30]A. B. Ustinov and G. Srinivasan, Tech. Phys. **55**(6), 900–903 (2010).

[31]X. Yang, Z. Zhou, and T. Nan, J. Mater. Chem. C **4**(2), 234–243 (2016).

[32]B. A. Belyaev, K. V. Lemberg, A. M. Serzhantov, A. A. Leksikov, Y. F. Bal'va, and A. A. Leksikov, IEEE Trans. Magn. **51**(6), 1–5 (2015).

[33]N. Chang, IEEE Trans. Magn. **18**(6), 1604–1606 (1982).

[34]D. Sharma, N. Khare, and M. P. Abegaonkar, Solid State Commun. **230**, 40–42 (2016).

[35]A. G. Gurevich and G. A. Melkov, *Magnetization Oscillations and Waves* (CRC Press, Boca Raton, 1996).

[36]J. Marsh, V. Zagorodnii, Z. Celinski, and R. E. Camley, Appl. Phys. Lett. **100**, 102404 (2012).

[37]A. M. Ferona and R. E. Camley, Phys. Rev. B **95**, 104421 (2017).

[38]B. Johansson, S. Haraldson, L. Pettersson, and O. Beckman, Rev. Sci. Instrum. **45**, 1445 (1974).

[39]B. A. Belyaev, A. A. Leksikov, A. M. Serzhantov, Y. F. Bal'va, and A. A. Leksikov, IEEE Trans. Plasma Sci. **42**(6), 1552–1559 (2014).

[40]B. A. Belyaev, A. V. Izotov, and A. A. Leksikov, IEEE Sens. J. **5**(2), 260–267 (2005).